Statistical characterization of Barkhausen noise

Kevin P. O'Brien and M. B. Weissman
Department of Physics, University of Illinois at Urbana-Champaign, 1110 West Green Street, Urbana, Illinois 61801-3080
(Received 13 May 1994)

We investigate whether Barkhausen noise exhibits self-organization and precursor events in the manner of the sandpile models used to illustrate self-organized criticality, and the extent to which Barkhausen noise can be described by single-domain wall pictures. Although a few large time-asymmetric events are found, no precursor effects were observed. Standard single-degree-of-freedom models appear to describe most of the data.

PACS number(s): 05.70.Ln, 75.60.Ej, 05.40.+j

INTRODUCTION

Recently, much attention has been focused on the hypothesis that nonequilibrium broadband noise in some driven systems can reflect a type of self-organization, in some cases producing a state with power-law correlations closely analogous to critical phenomena [1]. The original picture used to illustrate such models was of the cooperative flow of sand down a sloping pile, in which the local environment of each sand grain depends on the behavior of the neighboring sand grains. Although this approach, dubbed "self-organized criticality" (SOC), is quite appealing as an explanation for those temporal scaling phenomena not accounted for by the customary trivial explanations of $1/f$ noise [2], SOC has found surprisingly little direct experimental support, in part because inertial effects cause real sand to have a first-order dynamical transition. (See, e.g., [3].) Regardless of whether a particular driven system self-organizes to the analog of a critical state or to the analog of a first-order transition, even the simpler question of whether the distribution of characteristic times comes from simple fixed inhomogeneity or from some genuine self-organization remains open for most experimental systems.

Barkhausen noise, the irregular magnetization changes of a ferromagnet in a changing field, has been described as analogous to the noise of sand flow [4]. Recently, Barkhausen noise has been cited as a good experimental illustration of SOC, lacking inertial effects [5]. On the other hand, Barkhausen noise has been modeled as resulting from the motion of single-domain walls in a (one-dimensional) spatially rough coercive field created by defects [6]. Such a model is analogous to *individual* sand grains rolling down preexisting tilted rough surfaces, rather than collective motions of many sand grains generating their own random environments. The central question addressed in this paper is whether in Barkhausen noise we are hearing something like "the noise of sand grains falling over each other" [4] or like the sound of sand grains falling over something else.

BACKGROUND

Some of the ingredients of SOC are known to be potentially relevant to Barkhausen noise. In some cases, magnetization changes have been directly observed to occur via avalanche processes in the domain topology [7]. These avalanches exhibit some scaling effects, at least over a narrow range of parameters, and their behavior has been described by a subcritical self-organization model [8]. Also, the formation of multisegment magnetic domain walls in some cases has been described as self-organizing with some scaling properties [9].

The direct evidence cited for an SOC description of Barkhausen noise has consisted of a limited "scaling" regime in the spectral density of fluctuations in the induced Barkhausen voltage, $S(f)$ [5], together with some limited scaling of Barkhausen pulse sizes and times, and some correlation between those two variables [5]. Also, some very qualitative interpretations of wavelet decompositions have suggested that they have a "hierarchical" appearance, described as reminiscent of SOC [10].

For several reasons, there is no real evidence in the form of $S(f)$ for SOC effects. The first report of an apparent nontrivial spectral exponent [5] turned out to be based on an experimental artifact [5]. Even in quasiequilibrium, magnetic systems can show $1/f$ noise with beautiful spectral scaling [11], a reminder that scaling per se is not evidence of SOC.

Also, Barkhausen data (e.g., noise spectra) averaged over entire hysteresis loops can be misleading, since the properties at different parts of the hysteresis loop are not identical, as carefully shown by Alessandro *et al.* [12]. Lumping together data from different parts of a hysteresis loop can give spurious distributions in, for example, characteristic rates. Therefore, the existence of pulses with a range of sizes and durations should not be taken as conclusive evidence for SOC. In fact, such distributions are consistent with models with nothing resembling self-organization, in which many domains, each with its own coercive field, flip independently, although other evidence has shown that such models are too simplified to describe Barkhausen noise [13].

At least one key ingredient of realistic kinetic models of Barkhausen noise in metals is well established. The domain wall velocity is governed by eddy-current damping [14]. It is generally accepted that the resulting domain wall velocity is linear in the difference between the local magnetic field and a local coercive field due to defects in the material [6].

One class of Barkhausen models simply describes individual domain walls moving sequentially through spatially random coercive fields ($H_c(x)$) [6] (or, in some schematic models, random local magnetic fields [15]). Any scaling behavior shown by such individual-domain models reflects not self-organization but rather the scaling properties of the initial random field. For example, in a recent random-field model of hysteresis avalanche sizes show power-law scaling only when the random field magnitude is tuned to let the slope of the hysteresis loop approach infinity, without reaching a discontinuity [15].

In the most complete individual-domain-wall model, Alessandro *et al.* (ABBM) do consider interactions among different domain walls, but conclude that for their purposes a mean-field approximation of such effects is adequate [6]. Thus, their model explicitly ignores the cooperative effects which are necessary ingredients of SOC. Nevertheless, it manages to give a good approximation to experimental event-size distributions and spectra taken at a variety of different driving rates [12].

In fact, models of single-domain wall motion are known to be relevant to ordinary Barkhausen noise, since experiments in which only one domain wall was present produce noise qualitatively similar to ordinary Barkhausen noise [16,17]. Alessandro *et al.* [6] have shown that, for low driving rates, power-law scaling can be found in Barkhausen pulse sizes in simple single-wall, single-degree-of-freedom models, if the disordered coercive field is assumed to be described by a random walk, up to some correlation distance [6].

The description of $H_c(x)$ by a random walk in x is supported by data on noise from *single*-domain walls driven so as to maintain a constant rate of magnetization [16,17]. These data may be self-consistently interpreted as giving the one-dimensional spatial spectrum of the coercive field seen by a rigid domain wall [6]. If this interpretation is correct, then of course no form of self-organized theory is relevant. However, it may be that small-scale raggedness of the domain wall plays an important role [17], in which case self-organization of the many coupled degrees of freedom required to describe *one* wall could be important [9]. Such behavior would, of course, have little connection with the marginally stable domain topology observed under special circumstances [7,8].

Thus, it is unclear from previous data whether the spread of characteristic sizes and times in ordinary Barkhausen noise just directly reflects the heterogeneity of the domains and their pinning sites or actually involves cooperative avalanche processes of the type invoked in theories of dynamical self-organization. We have suggested that when self-organization due to external driving is important, the nonequilibrium nature of the kinetics should show up as violations of detailed balance, detectable directly in the time-dependence of the single measured variable [18]. For example, earthquake models show systematic small precursors to large events [19] and time records of a driven sandpile's mass in a recent experiment [20] showed precursor events without corresponding aftershocks.

On the other hand, many simple nonequilibrium processes, such as Barkhausen noise from a collection of independent domains each producing a pulse as it rotates at its own coercive field, would not show any such precursors, since a small event is equally likely to precede or follow a large one. The model of Alessandro *et al.* [6] (in the slow-driving limit) can be mapped by a simple transformation (using the square root of the domain-wall velocity rather than the velocity as the variable) to an ordinary one-dimensional equilibrium diffusion equation in a somewhat peculiar potential well. The steady-state solutions are therefore fully statistically time reversible and thus are qualitatively distinguishable from SOC behavior [18]. However, magnetic after effects can alter the equations of motion of the domain walls [21]. Such alterations can lead to time-irreversible behavior of the Barkhausen voltage.

When events on one scale systematically precede events on another scale, a time-asymmetric piece of certain fourth-order correlation functions (to be described) appears [18]. We found such a component in simulations of a simple 1D sand pile model [18]. In this paper, we shall investigate several higher-order statistical characterizations of Barkhausen noise for comparison with predictions of prior models. We focus on statistical characterizations involving both time correlations and amplitude distributions, since the simple time-correlation function and amplitude distribution function taken separately have already been shown to fit a single-degree-of-freedom model in soft magnetic metals [12]. We shall particularly emphasize the time symmetry of the fourth-order correlations.

EXPERIMENTAL TECHNIQUES

To investigate the SOC in Barkhausen noise, we used an amorphous iron-based metallic alloy (Metglass 2605TCA, obtained from Allied Signal), similar but not identical to the material used by Cote and Meisel [5]. This material comes in 30 μm thick splat-cooled sheets. The hysteresis loop, measured using a superconducting quantum interference device (SQUID) magnetometer, is shown in Fig. 1. The saturation field is around 100 Oe,

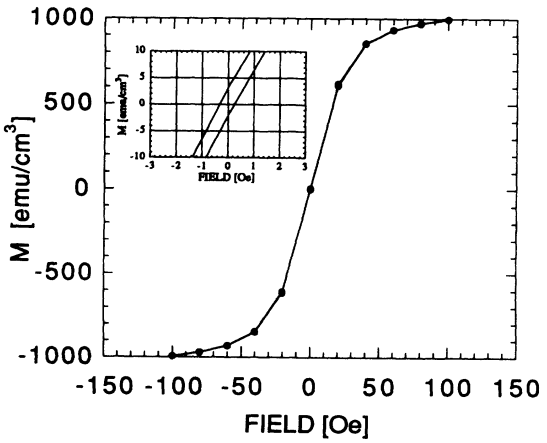

FIG. 1. The entire hysteresis loop, measured using a SQUID magnetometer The inset shows an enlargement of the hysteresis loop around zero field. The coercive width is about 0.4 Oe.

and the saturation magnetization is 1000 emu/cm^3. The width of the overall hysteresis loop is about 400 mOe. A minor loop, roughly corresponding to the field range used to measure the Barkhausen noise, has a width of ~ 50 mOe. There was no regime of infinite slope on the hysteresis loop.

To detect the Barkhausen noise, we wrapped a toroidal pickup coil (about 30 turns per cm) around a continuous annulus (inner diameter 2.4 cm, width 0.7 cm) cut from the Metglass sheet, allowing a continuous temporal measurement [13]. The time-dependent external field, with magnitude H_{ac}, was supplied by a small permanent magnet at a set distance from the toroid, sitting on a platform smoothly rotating at angular frequency Ω. The resulting field was predominantly in the plane of the Metglass annular sheet, and rotated at fixed magnitude as a function of time.

To reduce pickup noise and to ensure that the Metglass was being driven symmetrically through the hysteresis loop, we shielded the toroid and driving magnet inside a large μ-metal box. The background dc magnetic field was under 100 mOe. Standard low-noise voltage preamps were used. After antialias filtering (found to introduce negligible group delay differences in the frequency range of our measurements), the data was read into a computer via a 12 bit analog-to-digital convertor.

We used, in part, standard Fourier spectral analysis to describe the data. As we have argued previously, however, distinctions between different models usually require the use of non-Gaussian properties, measured in various higher moments of the fluctuations [2]. The most commonly used of such moments (in studying broadband noise) are a collection of fourth moments dubbed the second spectra, $S_2(f_2,f)$ and the cross second spectra, $S_2(f_2,f_a,f_b)$ [22]. $S_2(f_2,f)$ is obtained by repeatedly measuring $S(f)$ in a band around f, then treating the resulting time series of noise powers as the input to a low-frequency Fourier transform at frequencies f_2. (For broadband noise the bands about f are typically chosen to be octaves, since there is no structure in $S(f)$ on a finer scale.) $S_2(f_2, f_a, f_b)$ is obtained similarly, except that two time series of noise powers, around frequencies f_a and f_b are used. Their cross spectrum is obtained by taking the product of the Fourier transform of the time record of $S(f_a)$ and the complex conjugate of the Fourier transform of the record of $S(f_b)$. The time-asymmetric correlation functions showing systematic precursors show up as imaginary components of the cross second spectra [18]. All the second spectra presented are normalized by the product of the means of the power in the bands around f_a and f_b.

In the present experiment, certain limitations of this second spectral technique became awkward. The drawback of the Fourier technique is that, in collecting a set of complete first Fourier spectra, potential information about fast temporal variations of the power in the higher octaves of the first spectrum is discarded, in exchange for unused detailed spectral information. When, as in the current experiments, the entire spectral range from the lowest characteristic frequency of the system to the highest practical sampling rate is quite limited, it becomes necessary to take information with f_2 not too much less than f.

To measure the second spectrum in the potentially scaling regime, we instead used a wavelet transform for the first spectrum and a regular Fourier second spectrum. We used the extremely simple Haar discrete two-point wavelet transform [23]. The Haar transform is obtained by taking simple sums and differences of adjacent pairs of points. The differences give the highest-frequency data. Sums and differences of the pairwise sums are then taken. These differences give the next highest-frequency data, shifted down an octave in scale. The process is repeated until, at the last stage, the sum is simply the sum of all the data and the difference is the difference between the first and second half of the data. The Haar transform obviously provides poor frequency resolution together with good temporal resolution. It is very well suited to analysis of broadband noise, including Barkhausen pulses, for which greater frequency resolution is pointless.

We collect 120 arrays of 256 data points each. The Haar transform is then applied to each set of 256 points. The second spectrum is obtained via ordinary Fourier analysis of the squared-wavelet coefficients, which take the place of the octave sums of the older technique. (Care must be taken not to have any dead time between sequential sets of 256 points to assure proper timing of the second spectral data when the second spectral frequency extends above the lower range of the first spectral frequency, since the second transform includes several points from each of several sequential transforms.) All second spectra shown in this paper are taken by this method.

RESULTS

Barkhausen jumps with very ordinary appearance were found, as shown in Fig. 2. The large pulses typically had a magnitude of about 0.1 mV and a duration of about 0.2 msec. The corresponding change in magnetic moment of the sample is about 5×10^{-4} emu. Thus, the largest domain-wall motions sweep out about 5×10^{-7} cm^3 of volume, or about 2×10^{-4} cm^{-2} of area.

Figure 3 shows the Haar power spectrum compared to

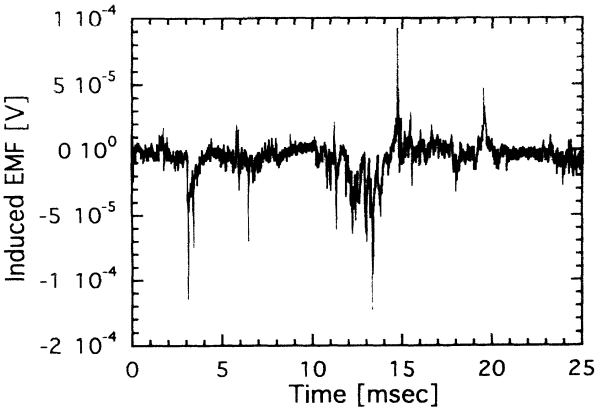

FIG. 2. Typical Barkhausen events are shown.

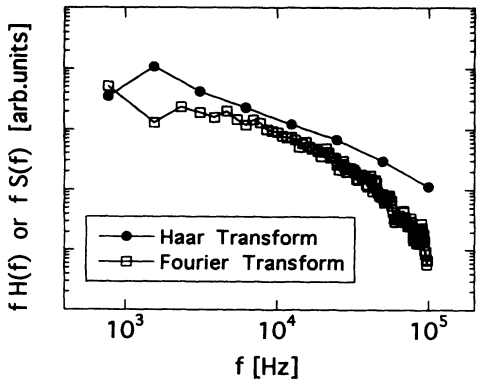

FIG. 3. The Haar and Fourier power spectra of the same 256 point data set.

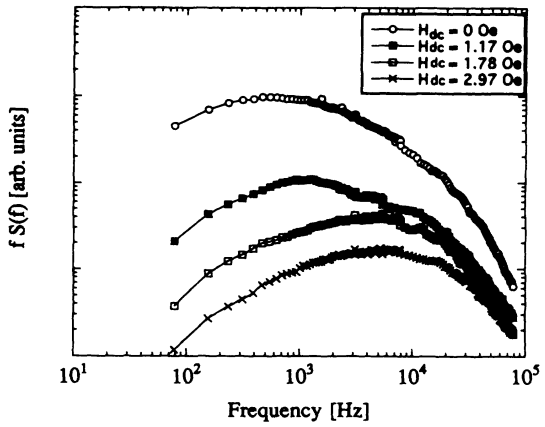

FIG. 5. Power spectra of the Barkhausen noise with $\Omega=0.5$ Hz and $H_{ac}=0.25$ Oe and varying H_{dc}.

the Fourier power spectrum of some of the Barkhausen data, illustrating the similarity of the two results, particularly in the frequency range for which $S(f)$ can be roughly approximated by a power law. $S(f)$ resembled that found in most other measurements of similar materials, looking roughly Lorentzian with a corner frequency near 100 Hz. The form of $S(f)$ depends only weakly on Ω, with the magnitude linear in Ω, as shown in Fig. 4, so we believe that the experiment is nearly in the slow-driving limit, suitable for comparison with simple theoretical models.

The portion of the hysteresis loop covered can affect $S(f)$ even for slow sweeps [12]. To investigate the effect of transversing other sections of the hysteresis loop, we put a dc magnetic field (H_{dc}) on the sample with a small permanent magnet. For higher H_{dc}, the crossover in $S(f)$ to the white noise regime moves to higher frequency, as seen in Fig. 5. The dc offset apparently results in a smaller cutoff to the size of the cascades. This result shows that it is inappropriate to describe the spectrum averaged over the entire hysteresis loop as if it were due to a stationary process with a set of scaling exponents. Some distribution of characteristic times would result simply from lumping together data taken at different fields. We see in Fig. 6 that changing H_{ac} at fixed H_{dc} has only a small effect on the form of $S(f)$ for $H_{ac}<4$ Oe, including the range used for our data. In the regime for which $S(f)\propto f^{-2}$ the ABBM picture would predict $S(f)\propto H_{ac}$, which is close to true of these data, although a slight deviation is noticeable for smallest value of H_{ac}.

Since the individual Barkhausen events are not the simple pulses of idealized SOC pictures, it is not obvious *a priori* how the Fourier content of a typical pulse falls off at high frequency. Therefore it is not obvious whether the high-frequency spectral shape is determined by the properties of individual pulses or by the overall distribution of pulse parameters [24]. The latter possibility has sometimes been assumed [5]. The covariance between the fluctuations in noise power in different frequency regimes provides a convenient tool to determine if those powers come from the same pulses or different ones.

As seen in Fig. 7, the fractional noise power variance does not begin to fall off substantially until f reaches

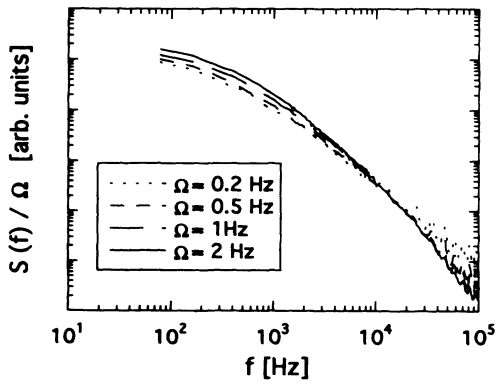

FIG. 4. The power spectrum of the Barkhausen noise for different Ω, driving magnet rotation rate. For all of the spectra $H_{ac}=0.5$ Oe and $H_{dc}=0$ Oe. As expected the noise power scales linearly with Ω.

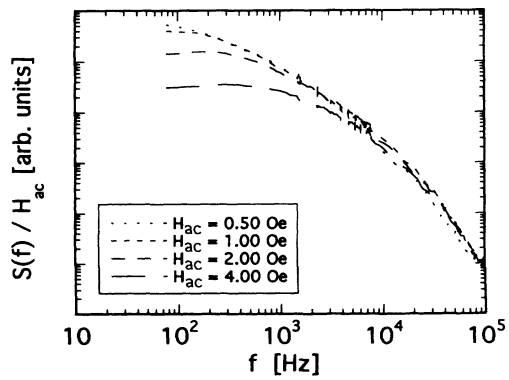

FIG. 6. Power spectra of the Barkhausen noise with $\Omega=0.5$ Hz and $H_{dc}=0$ and a varying H_{ac}. All of the spectra are divided by their respective H_{ac}.

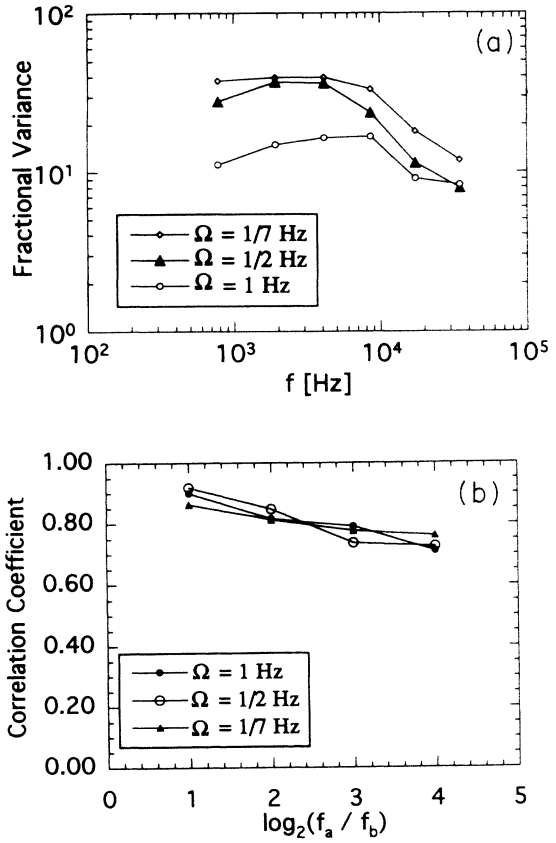

FIG. 7. (a) The fractional variance in the noise in different octaves is shown for several rotation rates. (b) The correlation coefficient for the noise power fluctuations is shown as a function of the ratio of the frequencies of the two bands.

~10 kHz, which is well into the regime in which the scaling has been attributed to the range of event sizes and durations. These fluctuations remain highly correlated for large octave separations, which means that the same set of pulses is giving most of the variance in the noise power over the entire observed frequency range. In itself, that fact does not demonstrate whether the high-frequency noise power itself (as opposed to its variance) comes mainly from big pulses. However, since the fractional variance only falls off about a factor of three over this range, the fraction of the noise power at 30 kHz which comes from pulses long enough to give most of the noise at 1 kHz cannot be much less than half. Thus, the spectral form is very far from being determined by the pulse size distribution in the regime of typical experiments.

The second spectra show large non-Gaussian effects. Each $S_2(f_2,f)$ is more than ten times larger than the Gaussian value. $S_2(f_2,f) \propto f_2^0$, similar to the sandpile simulations [18]. We sampled the voltage for the first spectrum at 200 kHz and for every set of parameters (H_{ac}, Ω and H_{dc}) we averaged at least 300 data runs.

We looked at a range of H_{ac}, Ω and H_{dc} parameters to find any imaginary piece in the second spectrum. The imaginary cross section spectra were small and of dubious statistical significance, although tending to be of the same sign as those found in sandpile simulations [18]. The largest effects were found when H_{ac} and Ω were small (0.25 Oe and 0.4 Hz in this case) and $H_{dc}=0$.

In Fig. 8, we show the real and imaginary parts of the second spectrum taken from the Haar first spectrum. The real part shows a white spectrum for f_2 within the range reached by our standard Fourier method, but with a rollover at higher f_2. The imaginary piece shows a clear deviation from zero for these high f_2. The imaginary piece reduces to zero at around 100 Hz, where the form of $S(f)$ crosses over to f^0. The sign of the imaginary part indicates that the fast events systematically precede the slow events, on average, as in the sandpile simulations [18].

These imaginary components of the cross second spectra are largest for the smallest Ω which we tried. They decreased rather rapidly at higher Ω, as illustrated in Fig.

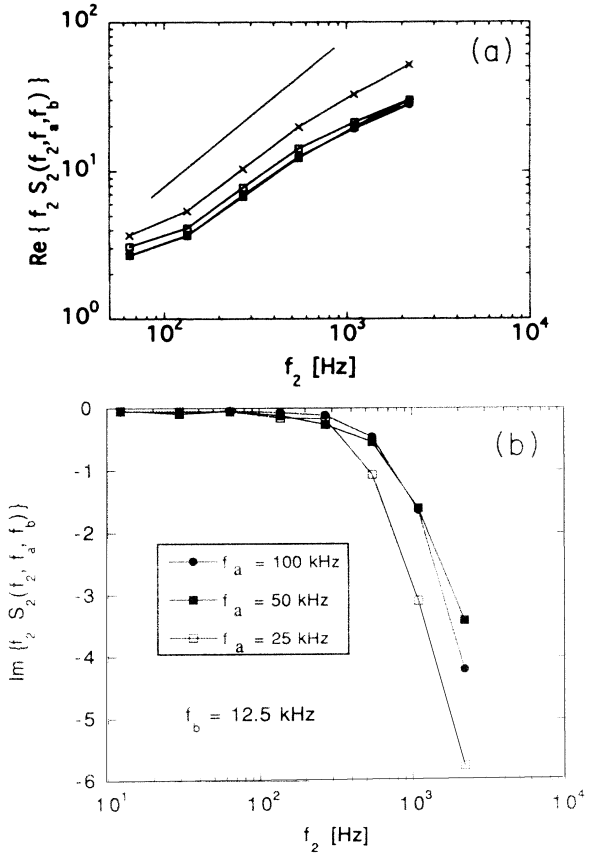

FIG. 8. Complex Fourier second spectra taken from a Haar first spectrum are shown. (a) is the real component, (b) imaginary. Both real and imaginary parts are normalized by the Gaussian expectation value for the real component. The sign convention for the imaginary component is that a negative value indicates that high-frequency noise precedes the low-frequency noise on that time scale. The imaginary cross second spectrum tends to zero at the same frequency the first spectrum flattens out to white noise. The straight line has slope of 1; it serves as a guide to the eye.

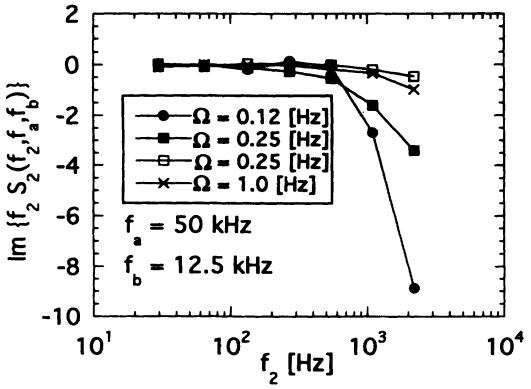

FIG. 9. The wavelet imaginary second spectrum [as in Fig. 8(b)] for different Ω. The imaginary components diminished for larger Ω.

9. Thus they do not result from departures from the slow-driving limit, and do not fit the ABBM model [6].

Inspection of segments of the data giving rise to imaginary cross second spectra shows that essentially the entire time asymmetry arises at rare events, as seen in Fig. 10, reminiscent of the large clusters of pulses which have been reported for some time [13]. About one second-spectral data set out of 100 shows these large asymmetrical events. Figure 11 illustrates the effect on the imaginary second spectrum of excising the event shown in Fig. 10. That single large event is the main contributor to the imaginary second spectrum. (The data used for Fig. 11 is separate run than that used for Fig. 9. The difference in size of the imaginary S_2 in these runs is consistent with statistical variation for a very small number of events.) There is no sign that the majority of small Barkhausen pulses are anything more complicated than individual domain walls moving in random environments.

The asymmetrical large pulses giving the imaginary S_2 all share a common appearance. They begin with a sharp voltage change, followed by a gradual return to zero. The return is often marked by smaller pulses. Although the asymmetrical pulses are mostly among the largest events observed, the largest symmetrical pulses are about as large.

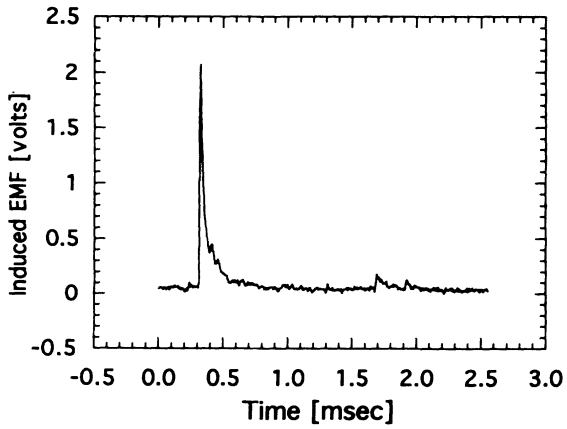

FIG. 10. The voltage trace of a large Barkhausen pulse that gives a large imaginary cross second spectrum.

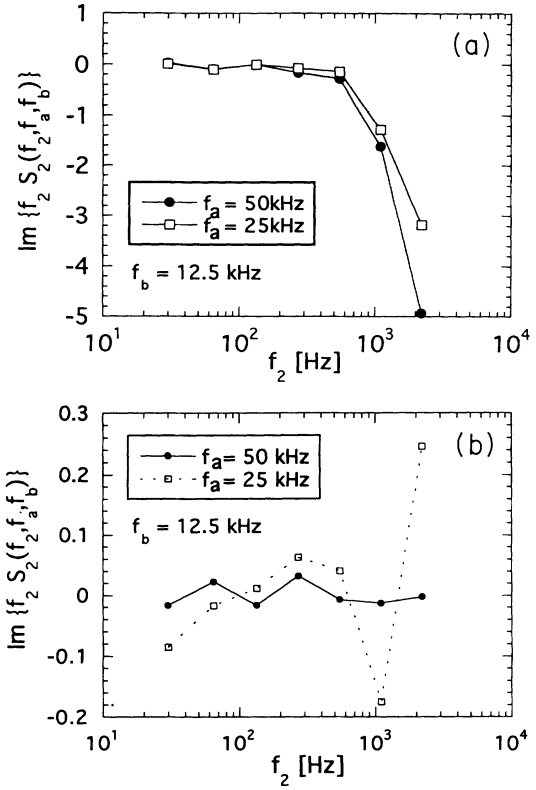

FIG. 11. (a) The imaginary second spectrum of the data set containing the pulse shown in Fig. 10. (b) The imaginary second spectrum of the data set after the pulse in Fig. 10 is removed. The imaginary component of the second spectrum is mainly caused by these rare large pulses.

CONCLUSION

The nontrivial scaling regime reported previously [5] as evidence for SOC in Barkhausen noise was not present in our data. Since the spectral form is consistent with simple single-degree-of-freedom models, there is no reason to describe the noise as critical. Most statistical characterization of the Barkhausen noise is consistent with the ABBM model.

However, using a wavelet transform to extend the frequency range of measurements of fourth-order correlation functions, we found clear time asymmetry in Barkhausen noise. In this respect Barkhausen noise differs sharply from most typical $1/f$ noise sources, which are usually found to be in quasiequilibrium [2,11]. More interestingly, it also differs from the simple versions of models of independently moving domain walls [6]. However, the time asymmetry was not due to precursor effects but rather to marked asymmetry of large, rare individual pulses.

Such pulses can be obtained in a very simple, physically plausible modification of the ABBM picture. If the coercive field contains a few strong-pinning spikes on top of a Gaussian random-walk background, then the domain wall will occasionally be abruptly stopped as it reaches such a site. However, the prior velocity will come from

the standard ABBM distribution and thus will usually be very small, so long as the driving rate is low. Each time the wall breaks loose from such a strong pinner, however, its velocity will suddenly jump to a large value, gradually decaying as the random-walk component of H_c catches up with H. (In fact, even a purely linear system will show similar-looking time asymmetries if driven with non-Gaussian spikes.)

The strong reduction in the strength of these asymmetrical events as the field sweep rate is increased indicates, however, that they cannot be modeled just as fixed spikes in the coercive field. Some time much longer than the largest correlation time of the Barkhausen spectrum is required to find these strong pinners. Two general possibilities arise. The time may be associated with magnetic after effects, i.e., structural relaxations in response to domain motion. Alternatively, the time may be associated with slow rearrangements of domain-wall segments (or even domain-wall topology) to settle into an optimally pinned pattern. Some such effect may have been anticipated in a remark by ABBM that the statistics of interactions among domain walls are expected to be important only for the low-frequency events [6]. Our future work will be directed toward sorting out these possibilities.

ACKNOWLEDGMENTS

This work was supported by NSF DMR 93-05763. We thank John Kelly for his very able technical assistance and Paul Fenimore for his assistance with the SQUID measurements. M. B. W. also thanks the Santa Fe Institute for holding an extremely helpful workshop.

[1] P. Bak, C. Tang, and K. Wiesenfeld, Phys. Rev. Lett. **59**, 381 (1987).
[2] M. B. Weissman, Rev. Mod. Phys. **60**, 537 (1988).
[3] S. R. Nagel, Rev. Mod. Phys. **64**, 321 (1992).
[4] R. P. Feynman, R. B. Leighton, and M. Sands in *The Feynman Lectures on Physics,* (Addison-Wesley, Reading, Feynman, MA 1964), Chapter 37, p. 9, "· · · the sudden changes of magnetization will produce impulses of emf in the coil, which are heard as distinct clicks in the loudspeaker. As you move the magnet nearer to the iron you will hear a whole rush of clicks which sound something like the noise of sand grains falling over each other as a can of sand is tilted."
[5] P. J. Cote and L. V. Meisel, Phys. Rev. Lett. **67**, 1334 (1991); L. V. Meisel and P. J. Cote, Phys. Rev. B **46**, 10 822 (1992). Note that our spectra, like most others in the literature, resemble those of the latter paper and not those of the Letter, in which aliasing was a problem.
[6] B. Alessandro, C. Beatrice, G. Bertotti, and A. Montorsi, J. Appl. Phys. **68**, 2901 (1990).
[7] K. L. Babcock and R. M. Westervelt, Phys. Rev. Lett. **64**, 2168 (1990).
[8] P. Bak and H. Flyvbjerg, Phys. Rev. A **45**, 2192 (1992).
[9] X. Che and H. Suhl, Phys. Rev. Lett. **64**, 1670 (1990).
[10] O. Geoffroy and J. L. Porteseil, J. Magn. Magn. Mater. **97**, 205 (1991).
[11] H. T. Hardner, M. B. Weissman, M. B. Salamon, and S. S. P. Parkin, Phys. Rev. B **48**, 16 156 (1993).
[12] B. Alessandro, C. Beatrice, G. Bertotti, and A. Montorsi, J. Appl. Phys. **68**, 2908 (1990).
[13] G. Montalenti and Z. Angew, Phys. **28**, 295 (1970).
[14] H. J. Williams, W. Shockley, and C. Kittel, Phys. Rev. **80**, 1090 (1950).
[15] J. P. Sethna, K. Dahmen, S. Kartha, J. A. Krumhansl, B. W. Roberts, and J. D. Shore, Phys. Rev. Lett. **70**, 3347 (1993).
[16] R. Vergne, J. C. Cotillard, and J. L. Porteseil, Rev. Phys. Appl. **16**, 449 (1981).
[17] W. Grosse-Nobis, J. Magn. Magn. Mater. **4**, 247 (1972).
[18] K. P. O'Brien and M. B. Weissman, Phys. Rev. A **46**, R4475 (1992).
[19] B. E. Shaw, J. M. Carlson, and J. S. Langer, J. Geophys. Res. **97**, 479 (1992).
[20] J. Rosendahl, M. Vekic, and J. Kelley, Phys. Rev. E **47**, 1401 (1993).
[21] C. Beatrice and G. Bertotti, J. Magn. Magn. Mater. **104-107**, 324 (1992).
[22] M. B. Weissman, Rev. Mod. Phys. **65**, 829 (1993).
[23] I. Daubechies, *Ten Lectures on Wavelets* (Society for Industrial and Applied Mathematics, Philadelphia, 1992).
[24] H. J. Jensen, K. C. Christensen, and H. C. Fogedby, Phys. Rev. B **40**, 7425 (1989).